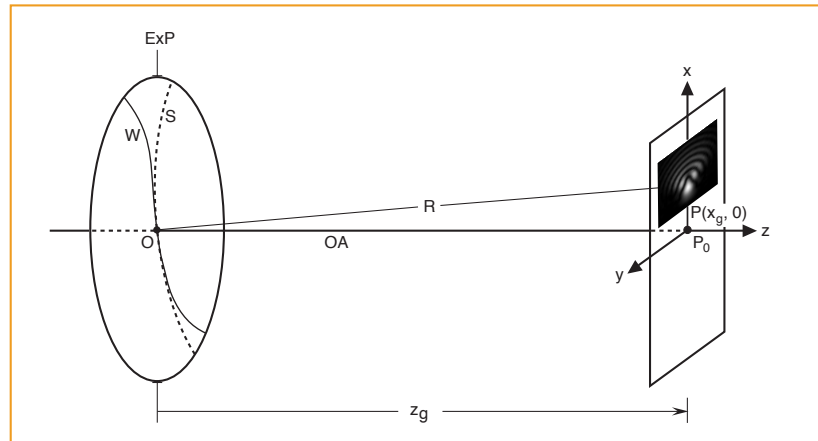


# Optical Imaging and Aberrations



© Virendra N. Mahajan

Adjunct Professor  
College of Optical Sciences  
University of Arizona

The Aerospace Corporation  
El Segundo, California 90245  
(310) 336-1783

virendra.n.mahajan@aero.org

## Lecture 9. Imaging With Circular Pupils:

Polychromatic PSF and OTF, Image of a Disc, Pinhole Camera,  
Two-Point Resolution

# Lecture 9 Summary

Polychromatic PSF and OTF, Image of a Disc, Pinhole Camera,  
Two-Point Resolution

- Polychromatic PSF
- Polychromatic OTF
- Image of a Disc
- Pinhole Camera
- Two-Point Resolution

## Polychromatic PSF

So far we have discussed monochromatic imaging by working at only one wavelength. Now we consider polychromatic imaging.

For simplicity, we assume aberration-free imaging.

### Monochromatic PSF:

$$I(r) = \left[ \frac{2J_1(\pi r)}{\pi r} \right]^2, \quad r \text{ in units of } \lambda F \text{ and } I \text{ in units of } \frac{P_{ex} S_{ex}}{\lambda^2 R^2} \text{ or } \frac{\pi P_{ex}}{4\lambda^2 F^2}$$

The PSF consists of a bright spot of radius 1.22 (in units of  $\lambda F$ ) surrounded by dark and bright diffraction rings.

The radius of the bright spot and the location of the diffraction rings depend on the wavelength of the object radiation.

For an object radiating in a wide spectral band, a diffraction pattern is formed at each wavelength with the result that the diffraction rings lose their sharpness---they smear out.

### Quasimonochromatic PSF (QPSF):

Let  $p$  be the image power per unit spectral bandwidth so that  $p\delta\lambda$  is the total image power in a very narrow spectral bandwidth  $\delta\lambda$ . QPSF may be written

$$I(r_i; \delta\lambda) = \frac{\pi p \delta\lambda}{4\lambda^2 F^2} \left[ \frac{2J_1(\pi r_i / \lambda F)}{\pi r_i / \lambda F} \right]^2, \quad I(0; \delta\lambda) = \frac{\pi p \delta\lambda}{4\lambda^2 F^2}$$

### Polychromatic PSF (PPSF):

Assume that an object radiates, the system images, and a sensor detects the image uniformly as a function of wavelength over a range from  $\lambda_1$  to  $\lambda_2$ .

$$\text{PPSF: } I(r_i; \Delta\lambda) = \frac{\pi p}{4F^2} \int_{\lambda_1}^{\lambda_2} \left[ \frac{2J_1(\pi r_i / \lambda F)}{\pi r_i / \lambda F} \right]^2 \frac{1}{\lambda^2} d\lambda$$

Spectral bandwidth:  $\Delta\lambda = \lambda_2 - \lambda_1$  , Mean wavelength:  $\lambda_m = (\lambda_1 + \lambda_2)/2$

$$\lambda_1 = \lambda_m \left( 1 - \frac{\Delta\lambda}{2\lambda_m} \right), \quad \lambda_2 = \lambda_m \left( 1 + \frac{\Delta\lambda}{2\lambda_m} \right)$$

Normalizing by the central value of the QPSF for a mean wavelength  $\lambda_m$ :

$$I_n(r_i; \Delta\lambda) = \frac{I(r_i; \Delta\lambda)}{I(0; \delta\lambda)} = \frac{\lambda_m^2}{\delta\lambda} \int_{\lambda_1}^{\lambda_2} \left[ \frac{2J_1(\pi r_i/\lambda F)}{\pi r_i/\lambda F} \right]^2 \frac{1}{\lambda^2} d\lambda$$

Normalized central value:

$$I_n(0; \Delta\lambda) = \frac{\lambda_m^2}{\delta\lambda} \int_{\lambda_1}^{\lambda_2} \frac{1}{\lambda^2} d\lambda = \frac{\lambda_m^2}{\delta\lambda} \left( \frac{1}{\lambda_1} - \frac{1}{\lambda_2} \right) = \frac{\Delta\lambda/\delta\lambda}{1 - (\Delta\lambda/2\lambda_m)^2} = \frac{10^4 \Delta\lambda/\lambda_m}{1 - (\Delta\lambda/2\lambda_m)^2}$$

Normalized wavelength:  $\lambda_n = \lambda/\lambda_m$  , normalized distance:  $r = r_i/\lambda_m F$

$$\frac{r_i}{\lambda F} = r \frac{\lambda_m}{\lambda} = \frac{r}{\lambda_n} , \quad \text{let } \frac{\delta\lambda}{\lambda_m} = 10^{-4} , \quad \therefore \frac{d\lambda}{\delta\lambda} = 10^4 d\lambda_n$$

$$I_n(r; \Delta\lambda) = \frac{4 \times 10^4}{\pi^2 r^2} \int_{1 - \frac{\Delta\lambda}{2\lambda_m}}^{1 + \frac{\Delta\lambda}{2\lambda_m}} J_1^2(\pi r/\lambda_n) d\lambda_n$$

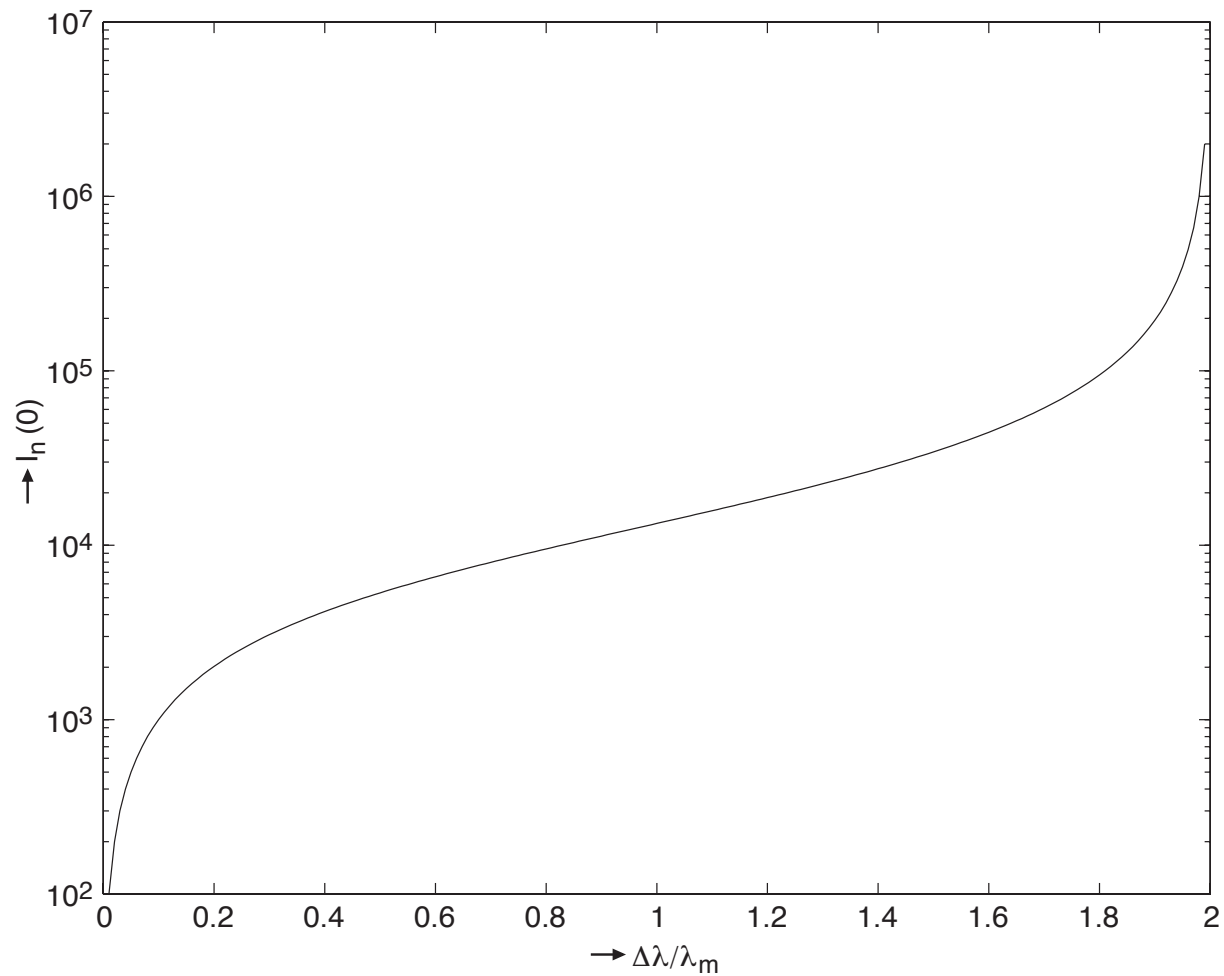


Figure 2-58a. Aberration-free central irradiance of the PPSF normalized by the central value of the QPSF as a function of the relative spectral bandwidth  $\Delta\lambda/\lambda_m$ .

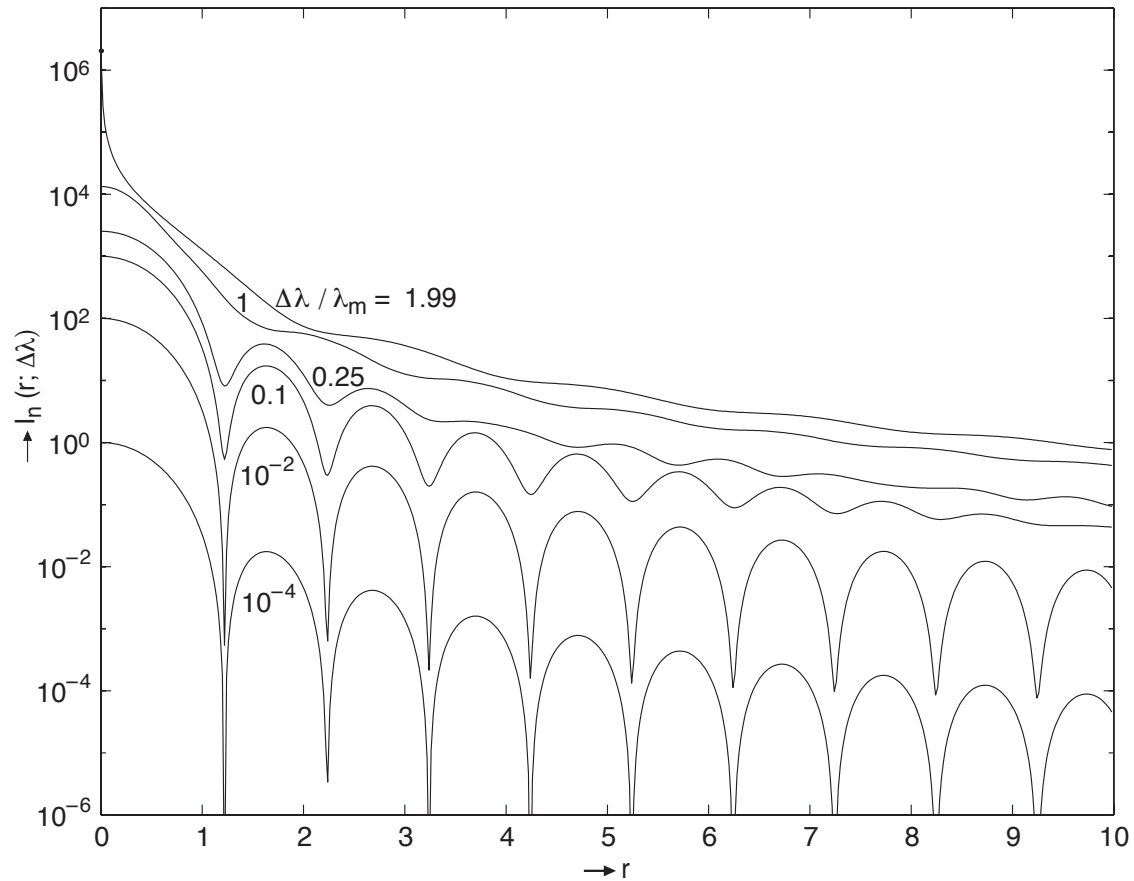


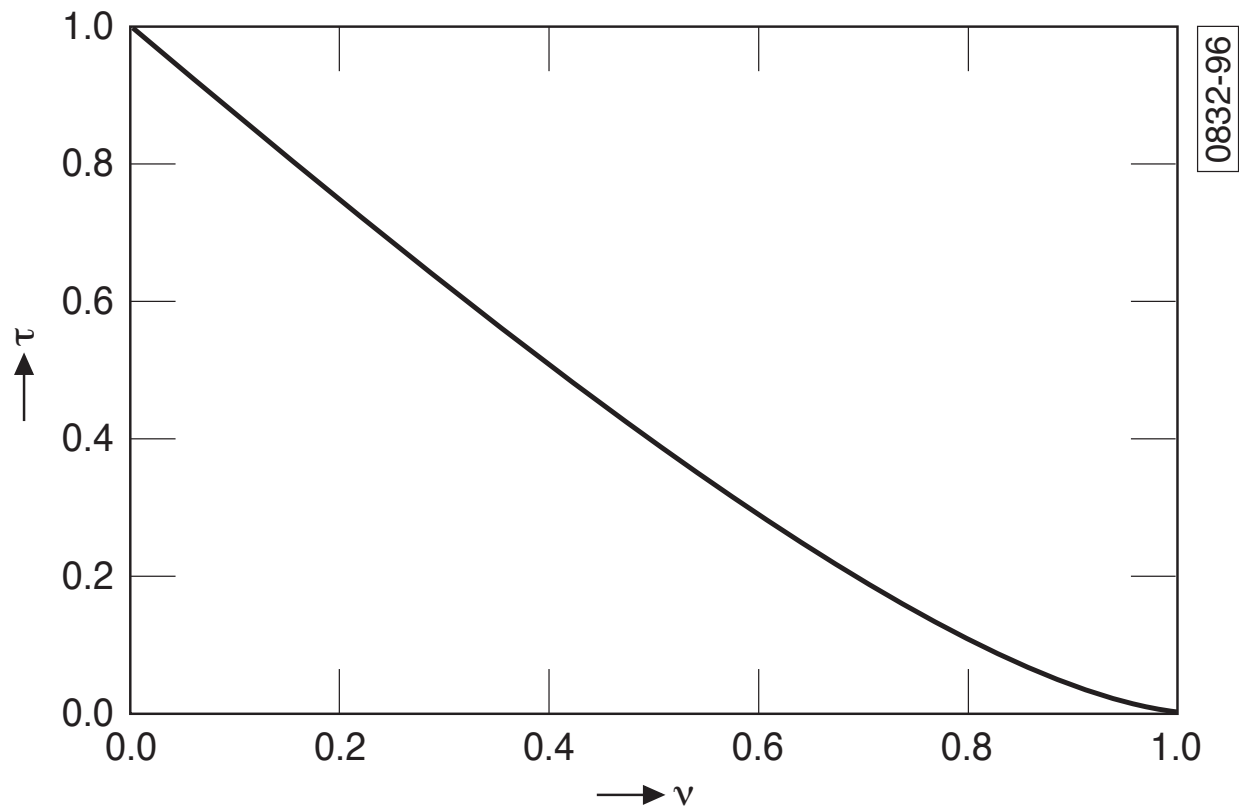
Figure 2-58b. Aberration-free PPSF for various relative spectral bandwidths  $\Delta\lambda/\lambda_m$ . The units of  $r$  are  $\lambda_m F$ .

- Ring structure does not disappear until  $\Delta\lambda/\lambda_m = 1$ , i.e., until the spectral bandwidth equals the mean wavelength.

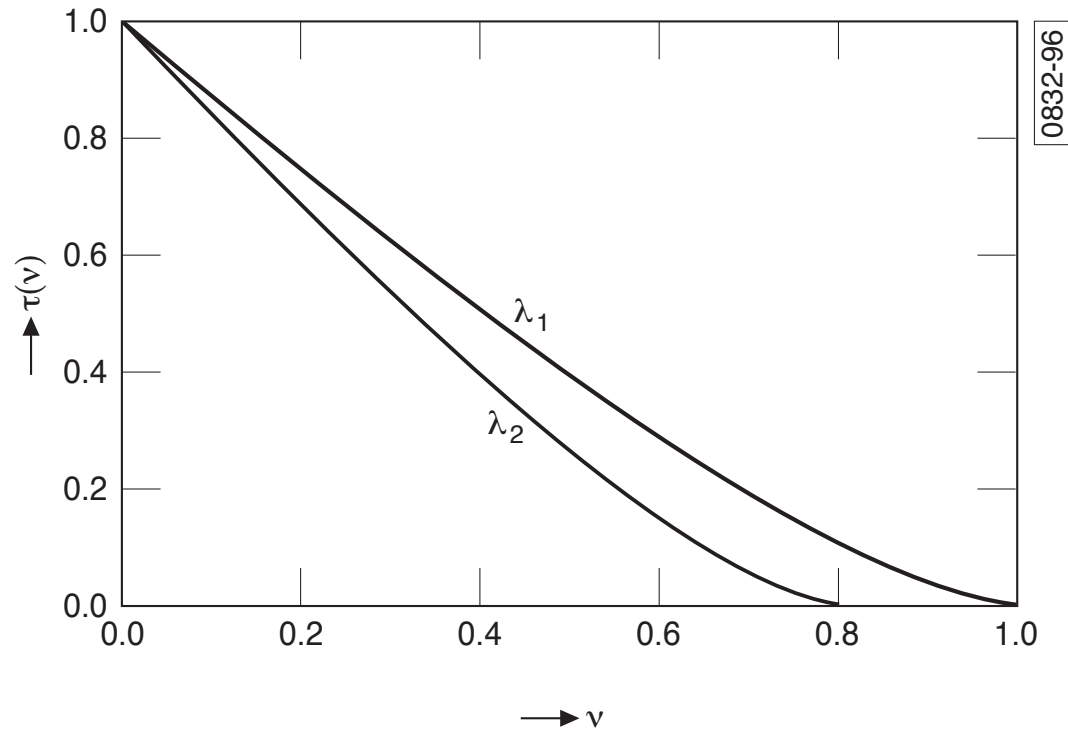
## Polychromatic OTF

### Monochromatic OTF:

$$\tau(v) = \frac{2}{\pi} \left[ \cos^{-1} v - v(1 - v^2)^{1/2} \right] \quad , \quad 0 \leq v \leq 1 \quad , \quad v = v_i / (1/\lambda F) = \lambda F v_i$$



## OTF at two wavelengths:



- The cut off frequency  $\nu_c = 1/\lambda F$  and the OTF for any frequency are higher for a shorter wavelength.
- If  $\lambda_1 < \lambda_2$ , then  $\nu_{1c} > \nu_{2c}$ , and the OTF is higher for  $\lambda_1$  than for  $\lambda_2$ .

## Polychromatic OTF:

$$\tau_p(v_i) = \frac{1}{\Delta\lambda} \int_{\lambda_1}^{\lambda_2} \tau(v_i) d\lambda = \frac{2}{\pi\Delta\lambda} \int_{\lambda_1}^{\lambda_2} \left[ \cos^{-1}(\lambda F v_i) - \lambda F v_i \left(1 - \lambda^2 F^2 v_i^2\right)^{1/2} \right] d\lambda$$

Let  $x = \lambda/\lambda_1$  ,  $q = \lambda_2/\lambda_1$  ,  $v = v_i/(1/\lambda_1 F)$

$$\therefore \frac{d\lambda}{\Delta\lambda} = \frac{\lambda_1 dx}{\lambda_2 - \lambda_1} = \frac{dx}{\left(\frac{\lambda_2}{\lambda_1} - 1\right)} = \frac{dx}{q-1} , \quad \lambda F v_i = \frac{\lambda}{\lambda_1} v = xv$$

$$\tau_p(v) = \frac{2}{\pi(q-1)} \int_1^q \left[ \cos^{-1}(xv) - xv \left(1 - x^2 v^2\right)^{1/2} \right] dx , \quad 0 \leq v \leq 1$$

- $q \leq 3$  because detectors respond to a relatively narrow spectral band.
- $q = 1$  for monochromatic ,  $q = \lambda_2/\lambda_1 = 0.7\mu\text{m}/0.4\mu\text{m} = 1.75$  for visible light.

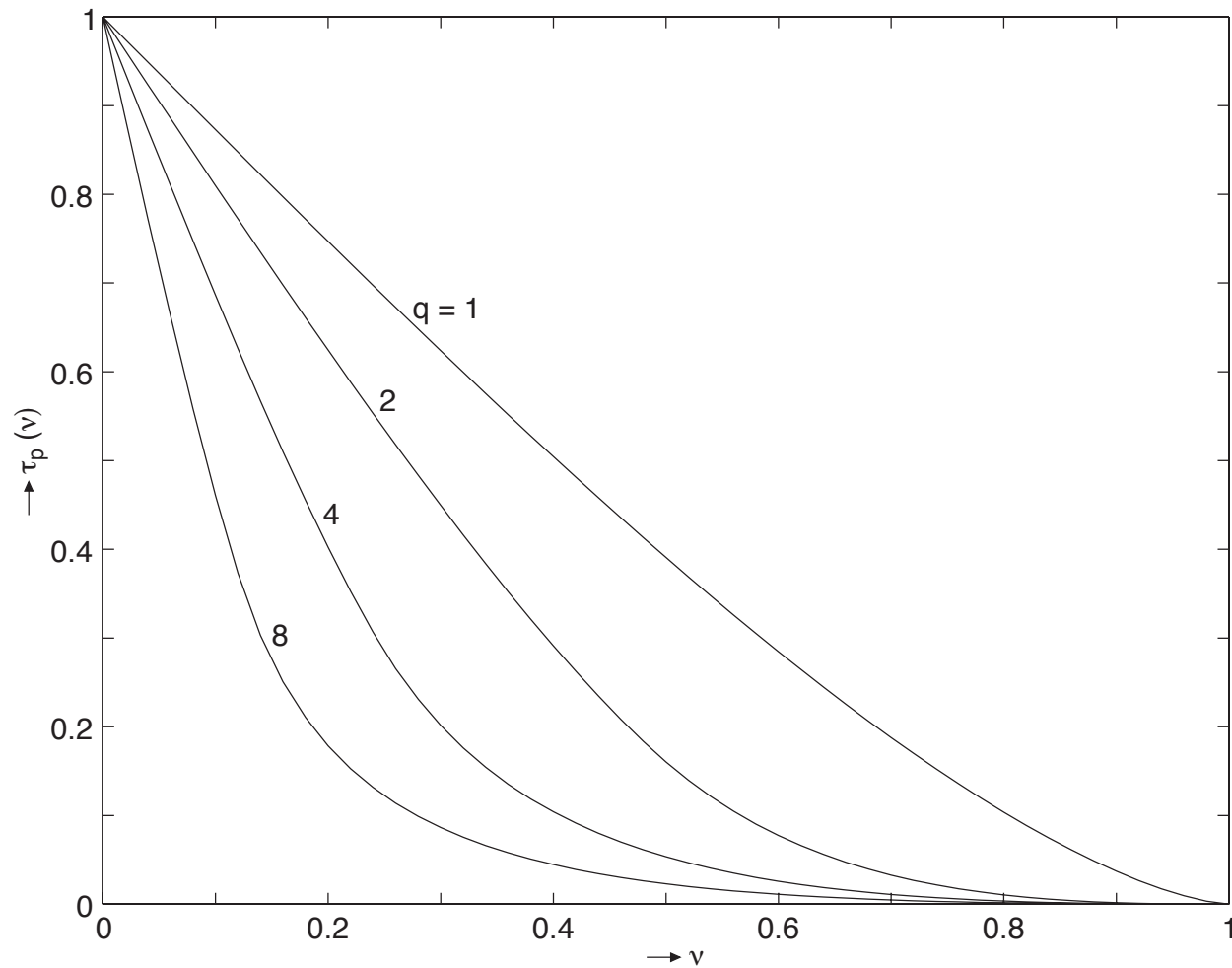


Figure 2-59. Polychromatic OTF of an aberration-free system.

- $\tau_p(\nu)$  decreases for all values of  $\nu$ , as  $q$  or spectral bandwidth increases.

## Image of an Incoherent Disc

As an example of the image of an *isoplanatic incoherent extended object*, we consider the image of a uniformly radiating or illuminated disc.

The diffraction image may be obtained by convolving the Gaussian image with the PSF or by inverse Fourier transforming its spatial frequency spectrum (which is equal to the product of the spectrum of the Gaussian image and the OTF).

- We want to determine the size of an object that can be treated as a point and thereby define the size of a pinhole that can be treated as a point source.

Consider an object that is a disc of radius  $h_o$  and radiance  $B$  lying at a distance  $z_o$  from the entrance pupil of area  $S_{en}$  of an imaging system.

First, we determine the Gaussian image, then the diffraction image by the convolution approach, and finally by the Fourier transform approach.

## Gaussian image:

Total power entering the system:

$$P_{en} = \pi h_o^2 \left( S_{en} / z_o^2 \right) B$$

Total power in the exit pupil and, therefore, in the image for a transmission factor  $\eta$ :

$$P_{ex} = \eta P_{en}$$

This power is uniformly distributed in the circular Gaussian image of radius

$$h_g = M h_o \quad , \quad \text{where } M \text{ is the image magnification}$$

Irradiance of the Gaussian image:

$$I_g(\vec{r}_g) = P_{ex} / \pi h_g^2 = \eta \left( S_{en} / z_o^2 M^2 \right) B = I_g \text{ for } |\vec{r}_g| \leq h_g$$

**Diffraction image** is *convolution* of the Gaussian image and the PSF:

$$\begin{aligned}
 I_i(\vec{r}_i) &= \int I_g(\vec{r}_g) PSF(\vec{r}_i - \vec{r}_g) d\vec{r}_g \\
 &= I_g \int PSF(\vec{r}_i - \vec{r}_g) d\vec{r}_g \quad , \quad |\vec{r}_g| \leq h_g
 \end{aligned}$$

Aberration-free image:

$$PSF(\vec{r}_i) = \frac{S_{ex}}{\lambda^2 R^2} \left[ \frac{2J_1(\pi r_i / \lambda F)}{\pi r_i / \lambda F} \right]^2$$

$$I_i(\vec{r}_i) = \frac{I_g S_{ex}}{\lambda^2 R^2} \int_0^{h_g} \int_0^{2\pi} \left[ \frac{2J_1(\pi s / \lambda F)}{\pi s / \lambda F} \right]^2 r_g dr_g d\theta_g$$

$$s = |\vec{r}_i - \vec{r}_g| = \left[ r_i^2 + r_g^2 - 2r_i r_g \cos(\theta_i - \theta_g) \right]^{1/2}$$

- Image is radially symmetric, as expected, since functional dependence on  $\theta_i$  disappears when  $\theta_g$  integration is carried out; indeed we may let  $\theta_i = 0$ .

Let  $r = r_i/\lambda F$ ,  $\rho_g = r_g/\lambda F$ ,  $b_g = h_g/\lambda F$  and  $t = s/\lambda F = \left(r^2 + \rho_g^2 - 2r\rho_g \cos\theta_g\right)^{1/2}$

$$I_i(r) = \frac{\pi I_g}{4} \int_0^{b_g} \int_0^{2\pi} \left[ \frac{2J_1(\pi t)}{\pi t} \right]^2 \rho_g d\rho_g d\theta_g$$

This is a cumbersome double integration, first over  $\theta_g$  and then over  $\rho_g$ . The integration is simpler in the frequency domain.

Central irradiance:

$$I_i(0) = I_g \int_0^{b_g} \frac{2J_1^2(\pi\rho_g)}{\rho_g} d\rho_g = I_g \left[ 1 - J_0^2(\pi b_g) - J_1^2(\pi b_g) \right] \quad (2-280)$$

- *Variation of  $I_i(0)$  with  $b_g$  is similar to the variation of the encircled power of the Airy pattern. It approaches  $I_g$  asymptotically.*

## Diffraction image in the spatial frequency domain:

Spectrum of the image is equal to the product of the spectrum of the Gaussian image and the OTF  $\tau(\vec{v}_i)$ . Inverse Fourier transform of the spectrum yields the image.

Since the Gaussian image is radially symmetric, its spectrum is given by its zero-order Hankel transform:

$$I_g(\vec{v}_i) = 2\pi I_g \int_0^{h_g} J_0(2\pi v_i r_g) r_g dr_g = (I_g h_g / v_i) J_1(2\pi v_i h_g) = P_{ex} \frac{2J_1(2\pi v_i h_g)}{2\pi v_i h_g}$$

Image spectrum:

$$I_i(\vec{v}_i) = I_g(\vec{v}_i) \tau(\vec{v}_i) = P_{ex} \frac{2J_1(2\pi v_i h_g)}{2\pi v_i h_g} \tau(\vec{v}_i)$$

Image:

$$I_i(\vec{r}_i) = \int I_i(\vec{v}_i) \exp(-2\pi i \vec{v}_i \cdot \vec{r}_i) d\vec{v}_i = I_g h_g \int (1/v_i) J_1(2\pi v_i h_g) \tau(\vec{v}_i) \exp(-2\pi i \vec{v}_i \cdot \vec{r}_i) d\vec{v}_i$$

**Very small disc**, i.e., for very small values of  $b_g$ , e.g., a pinhole,

$$J_1(2\pi v_i h_g) \simeq \pi v_i h_g \quad (2-292)$$

$$\therefore I_i(\vec{r}_i) = I_g(\pi h_g^2) \int \tau(\vec{v}_i) \exp(-2\pi i \vec{v}_i \cdot \vec{r}_i) d\vec{v}_i = P_{ex} \int \tau(\vec{v}_i) \exp(-2\pi i \vec{v}_i \cdot \vec{r}_i) d\vec{v}_i$$

or  $I_i(\vec{r}_i) = P_{ex} PSF(\vec{r}_i)$  (as expected for a point object)

**Radially symmetric aberration:** FT reduces to zero-order Hankel transform

$$I_i(r_i) = P_{ex} PSF(r_i) = 2\pi P_{ex} \int \tau(v_i) J_0(2\pi v_i r_i) v_i dv_i$$

Encircled power in a circle of radius  $r_c$ :

$$\begin{aligned} P_i(r_c) &= 2\pi \int_0^{r_c} I_i(r_i) r_i dr_i = (2\pi)^2 P_{ex} \int \tau(v_i) v_i dv_i \int_0^{r_c} J_0(2\pi v_i r_i) r_i dr_i \\ &= 2\pi r_c P_{ex} \int \tau(v_i) J_1(2\pi v_i r_c) dv_i \\ &= P_{ex} \left[ 1 - J_0^2(\pi r_c) - J_1^2(\pi r_c) \right] \quad (\text{for aberration-free imaging}) \end{aligned}$$

## Large disc and radially symmetric aberration:

$$I_i(r_i) = 2\pi I_g h_g \int J_1(2\pi v_i h_g) J_0(2\pi v_i r_i) \tau(v_i) dv_i$$

Let  $r = r_i/\lambda F$  and  $v = v_i/(1/\lambda F)$

$$\therefore I_i(r) = 2\pi I_g b_g \int_0^1 J_1(2\pi v b_g) J_0(2\pi v r) \tau(v) dv$$

$$I_i(0) = 2\pi I_g b_g \int_0^1 J_1(2\pi v b_g) \tau(v) dv$$

$$= I_g P(b_g)$$

$$= I_g \left[ 1 - J_0^2(\pi b_g) - J_1^2(\pi b_g) \right] \quad (\text{for aberration-free imaging})$$

Power in a circle of radius  $r_c$  (in units of  $\lambda F$ )

$$\begin{aligned}
 P_i(r_c) &= (2\pi)^2 I_g b_g \int_0^1 J_1(2\pi\nu b_g) \tau(\nu) d\nu \int_0^{r_c} J_0(2\pi\nu r) r dr \\
 &= 2P_{ex} \frac{r_c}{b_g} \int_0^1 J_1(2\pi\nu b_g) J_1(2\pi\nu r_c) \tau(\nu) (1/\nu) d\nu
 \end{aligned}$$

- Much simpler to calculate  $I_i(r)$  or  $P(r_c)$  by substituting the value of  $\tau(\nu)$ .

Power in a circle whose radius is equal to that of the Gaussian image:

$$P_i(b_g) = 2P_{ex} \int_0^1 J_1^2(2\pi\nu b_g) \tau(\nu) (1/\nu) d\nu \quad (2-289)$$

Relation between the power  $P(r_c; b_g)$  in a circle of radius  $r_c$  due to a source of radius  $b_g$  and the power  $P(b_g; r_c)$  in a circle of radius  $b_g$  due to a source of radius  $r_c$ :

$$b_g^2 P(r_c; b_g) = 2r_c b_g \int_0^1 J_1(2\pi\nu b_g) J_1(2\pi\nu r_c) \tau(\nu) (1/\nu) d\nu = r_c^2 P(b_g; r_c) \quad (2-291)$$

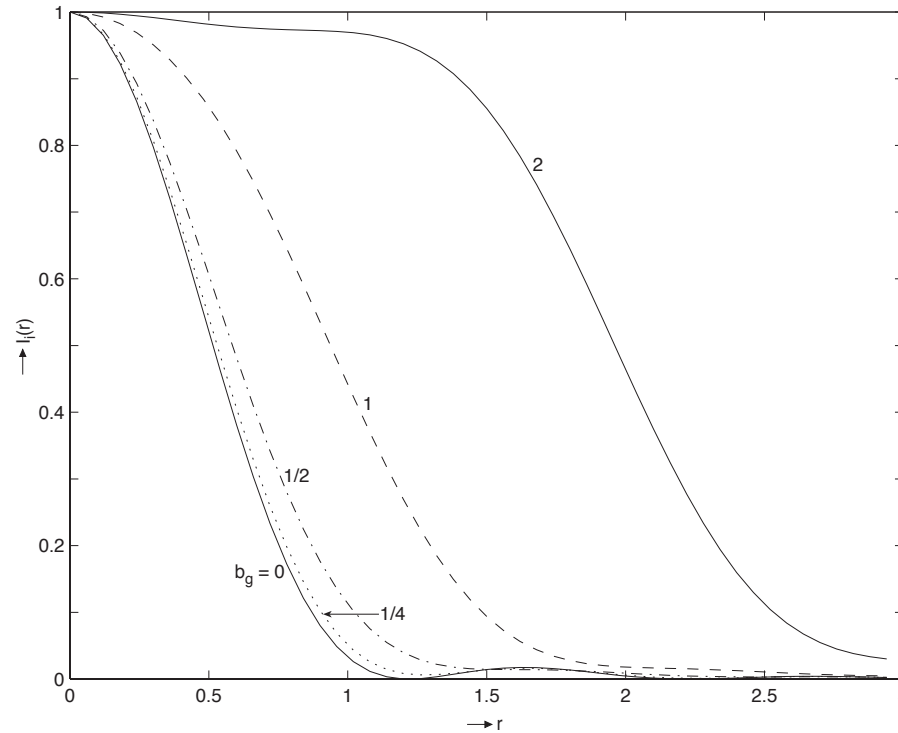


Figure 2-60. Normalized aberration-free image of an incoherent disc whose Gaussian image has a radius of  $b_g$ .  $r$  and  $b_g$  are in units of  $\lambda F$ .

- The image of an object whose Gaussian image radius  $b_g = 1/4$  (in units of  $\lambda F$ ) is approximately the same as the Airy pattern. Hence, such an object can be treated as a point.
- Similarly, a *pinhole with  $b_g = 1/4$  can be treated as a point source.*

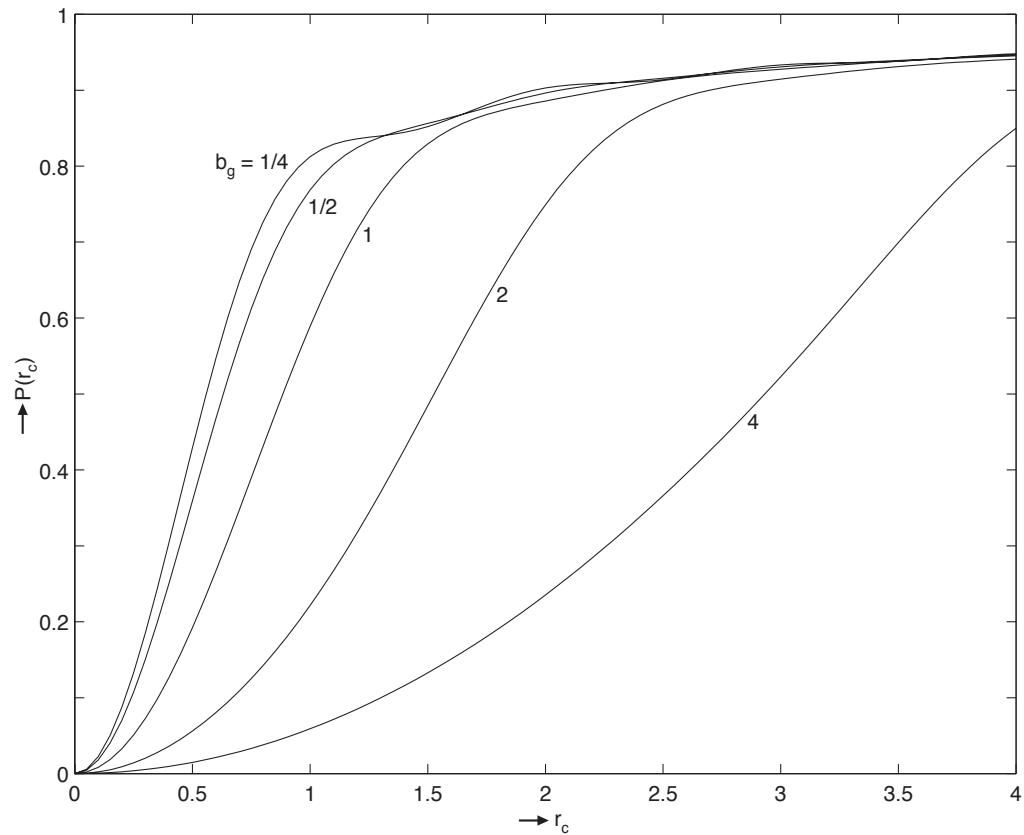


Figure 2-61a. Encircled power of the aberration-free image of an incoherent disc normalized by the total power  $P_{ex}$ .  $r_c$  is in units of  $\lambda F$ .

- $P(r_c)$  for the aberration-free image of a disc for  $b_g = 1/4$  closely resembles the encircled power of the Airy pattern, confirming the size of a pinhole that can be treated as a point source.

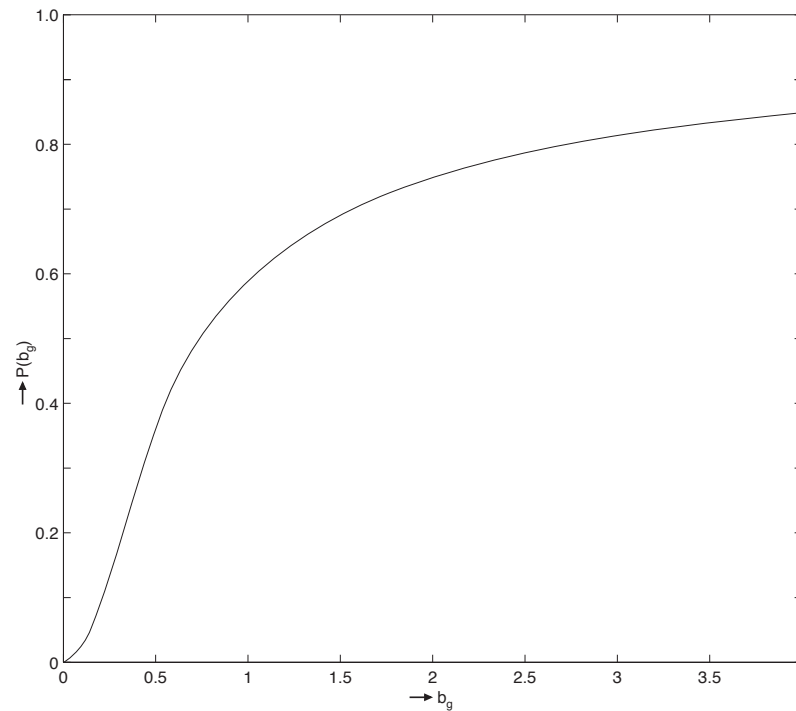


Figure 2-61b. Power in a circle of radius equal to that of the Gaussian image of the disc as a function of its size.

- $P(b_g)$  increases monotonically as the disc size increases.
- $P(b_g)$  for small values of  $b_g$  contains only a small fraction of the total power, since it is spread by diffraction.
- $P(b_g)$  for  $b_g \gg \lambda F$  contains a significant fraction of the total power, since the effect of diffraction for large objects is relatively small.

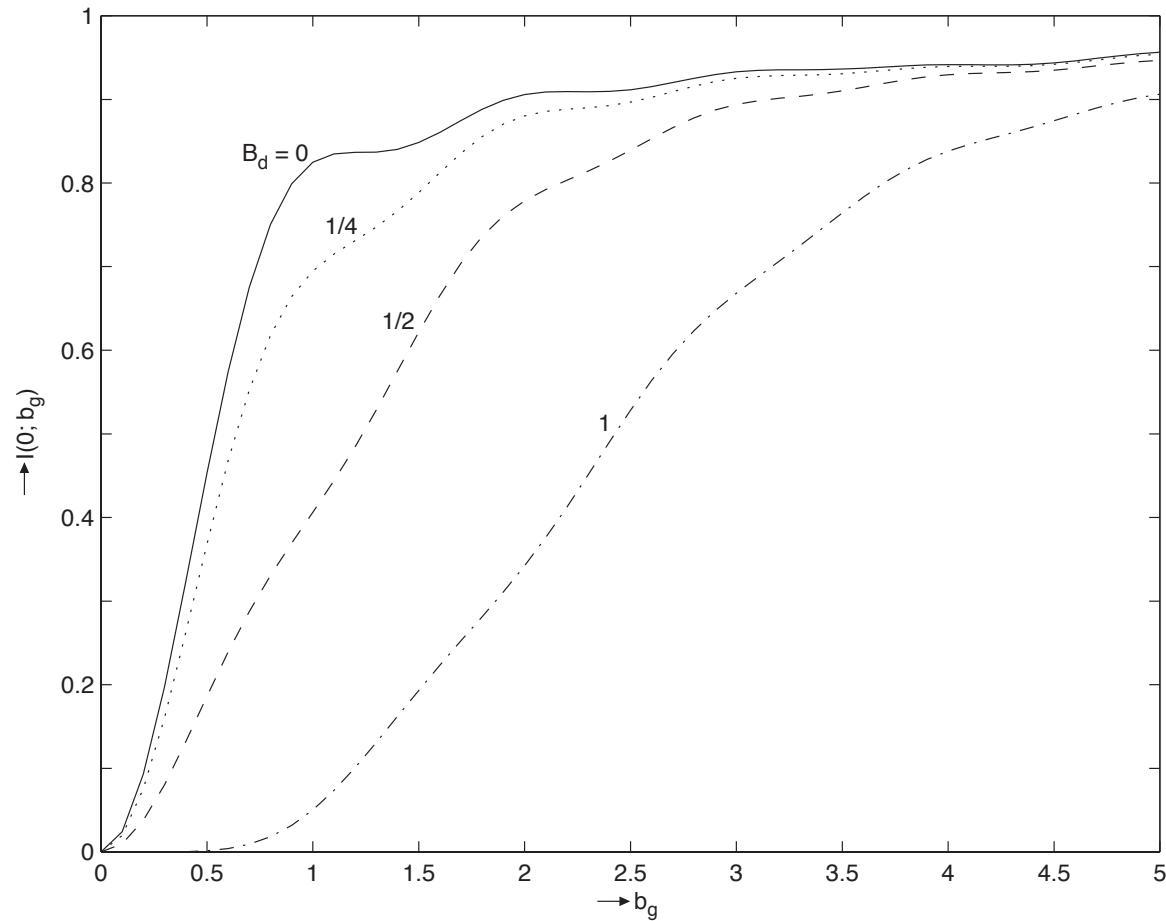


Figure 2-62a. Central irradiance of a *defocused image* of an incoherent disc.

- Central irradiance approaches unity (actually  $I_g$ ) asymptotically.

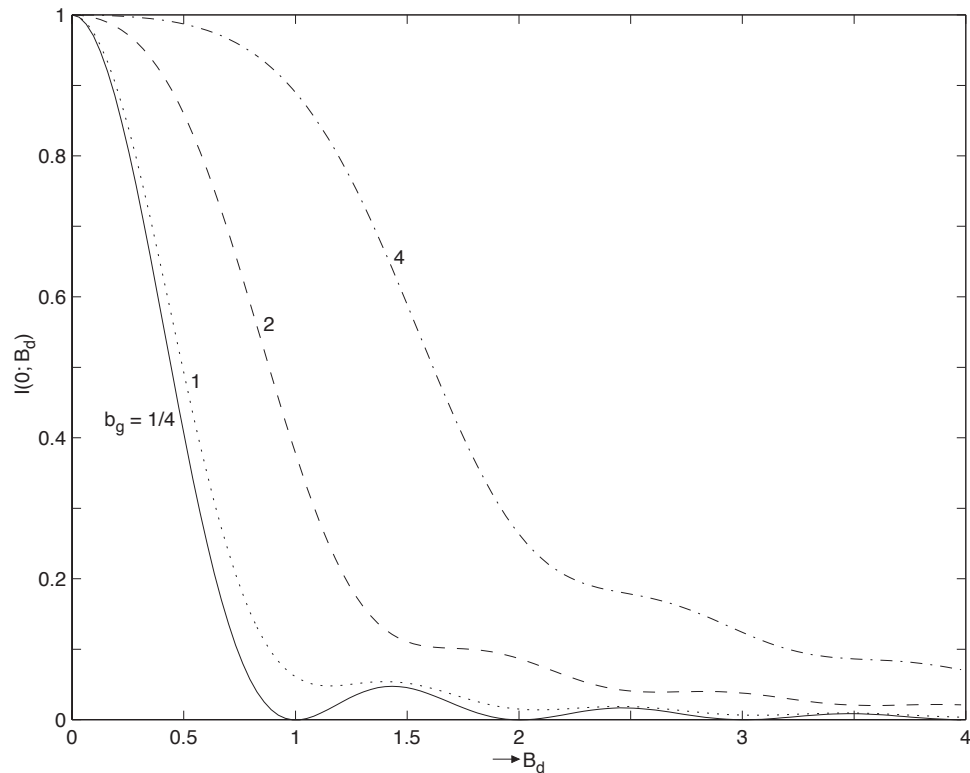


Figure 2-62b. Axial irradiance of a defocused image of an incoherent disc normalized to unity at the center. The actual central values (normalized by  $I_g$ ) in increasing order of  $b_g$  are 0.14, 0.825, 0.91, and 0.94.

- For  $b_g = 1/4$ , axial irradiance is approximately the same as for a point source. For example, it is nearly zero for integral values of  $B_d$  (in units of  $\lambda$ ). It becomes nonzero for larger discs.

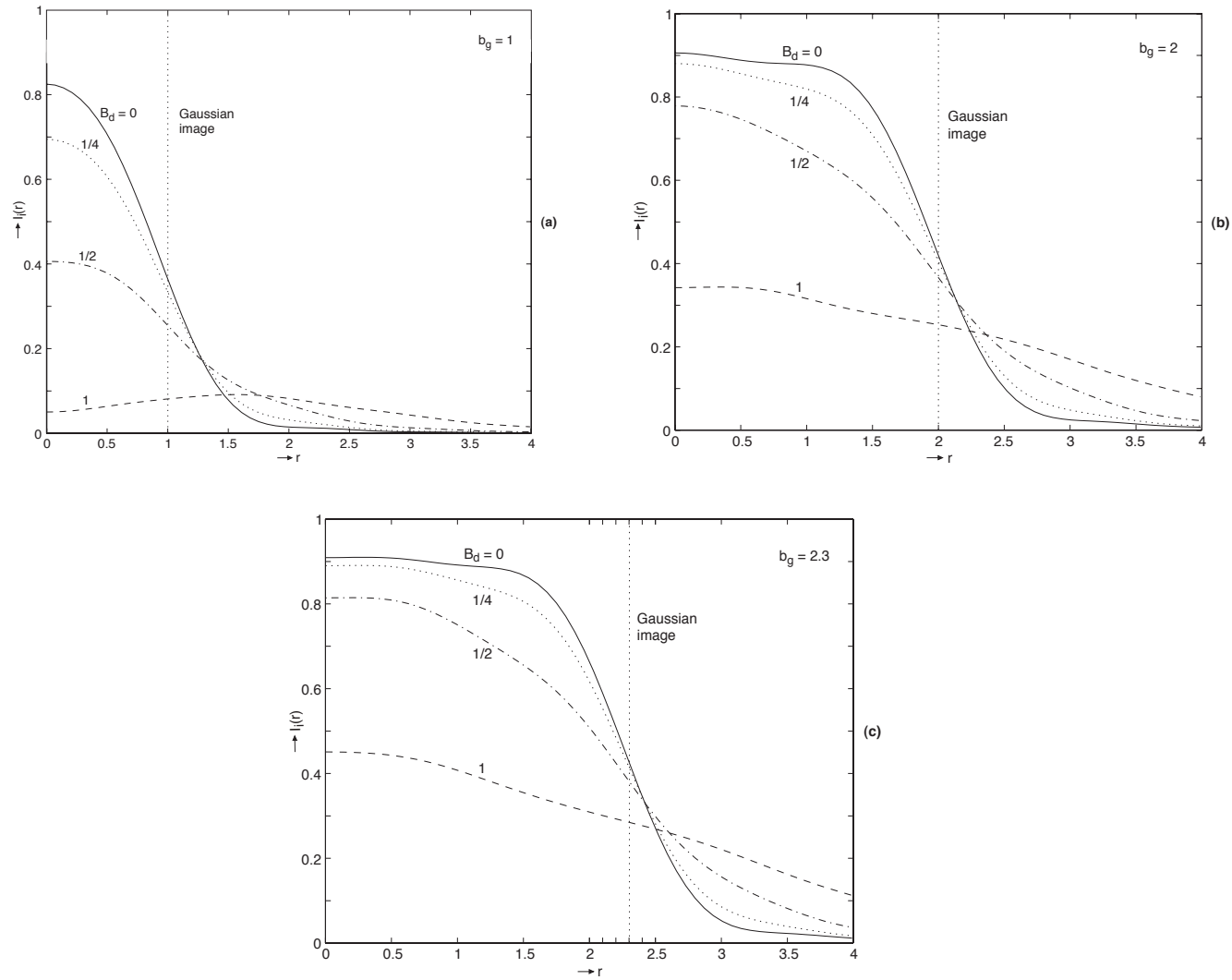


Figure 2-63. Irradiance distribution of defocused images of an incoherent disc. Gaussian image of radius  $b_g$  is indicated by the dashed vertical line.

The image generally resembles the object. In particular, it is bright in the central region and dim in the outer region.

- As defocus increases, the irradiance decreases in the central region and increases in the outer region.
- If the disc is small and the defocus is large, the irradiance at the center may be smaller than that in the outer region as, for example, for  $b_g = 1$  and  $B_d = 1\lambda$ . This behavior is similar to that for a point source, and it disappears as the disc size increases.
- The central irradiance of the image of a *coherently* illuminated disc can be much lower than that in the surrounding region, whether or not the image is defocused (unless the disc is very small like a point object). Moreover, defocus can increase the central irradiance (see Figures 2-76 and 2-77 on pp. 236-237).

## Pinhole Camera

- A pinhole camera (or camera obscura) has been the subject of many investigations, including those by Petzval and Rayleigh.
- It is simple (a pinhole of radius  $a$  on one side of a box of length  $L$  and the film on the other), *distortion free* with an *infinite depth of field* and a *very wide field of view*.

### **Petzval approach for a relationship between $a$ and $L$ (1857):**

- The geometrical image of a distant point object is approximately the same size as the pinhole if the pinhole is large.
- Reducing the pinhole size reduces the image size until diffraction by the pinhole spreads it.
- Optimum image is obtained by *minimizing the image spot radius* representing the sum of the geometrical and diffraction contributions to it.

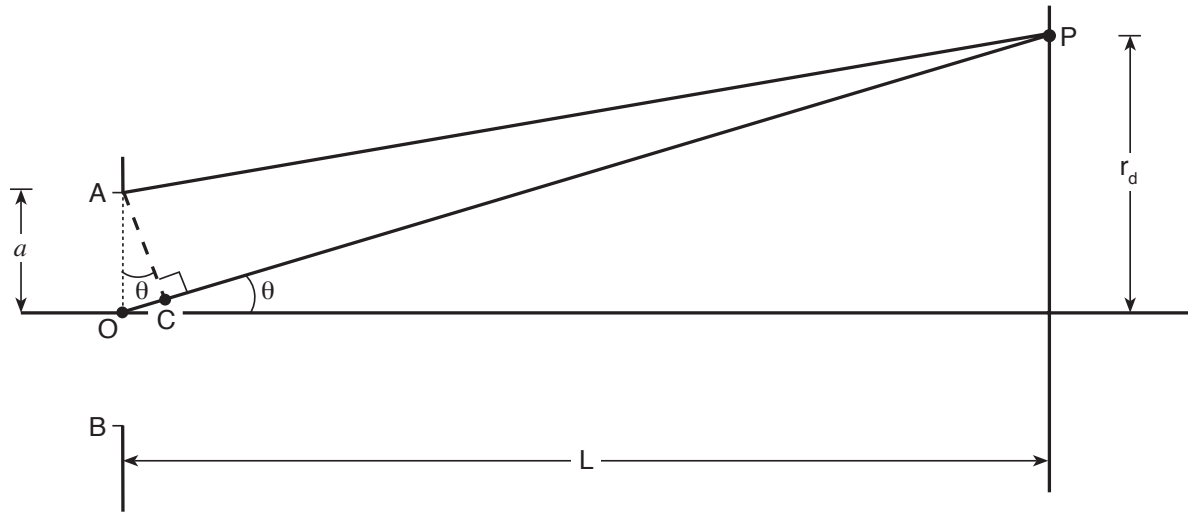


Figure 2-64. Diffraction spot radius based on the cancellation of disturbances from the center and the edge of a pinhole.  $L \gg a$

- Diffraction image radius is approximately equal to the distance of a point  $P$  from the center of the image at which a disturbance from the center  $O$  of the pinhole cancels that from its edge  $A$ , i.e., when

$$OP - AP = OC = \lambda/2$$

- Diffraction spot radius:

$$r_d = L\theta = L(OC/a) = \lambda L/2a$$

- Adding the geometrical and diffraction contributions, we obtain the image spot radius as

$$r_i = a + \lambda L / 2a$$

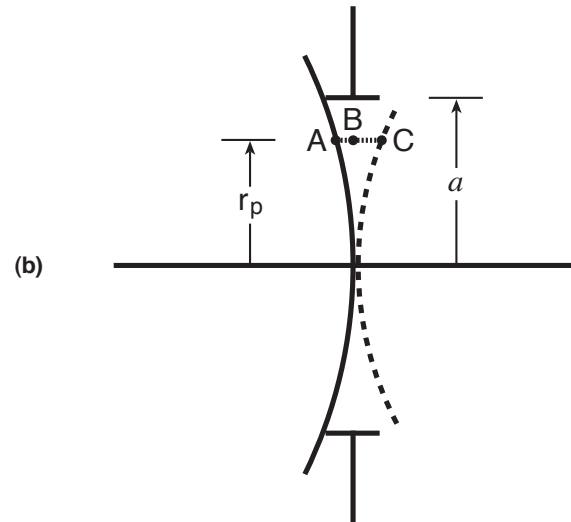
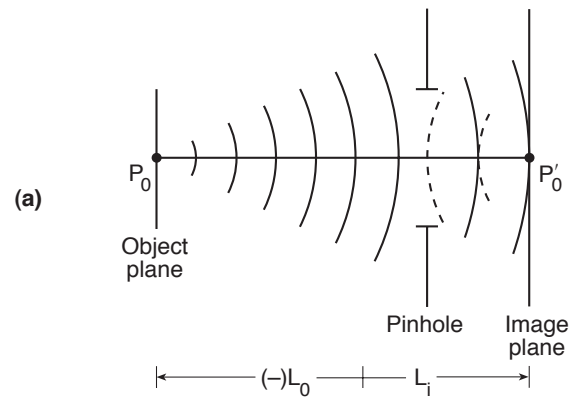
- Differentiating with respect to  $a$  and equating the result to zero, we obtain the optimum pinhole radius

$$a_P = \sqrt{\lambda L / 2}$$

$$\therefore r_i = 2a_P = \sqrt{2\lambda L} \quad (2-298)$$

### **Defocus aberration tolerance approach:**

- The difference between a pinhole camera and a regular camera is that the former does not use a lens to form the image.
- The lens in a regular camera converts a diverging spherical wave from a point object  $P_0$  into a spherical wave converging to an image point  $P'_0$  in the image plane.



(a) Imaging by a **pinhole camera** of radius  $a$ . (b) Wavefront incident on the pinhole and emerging wavefront (shown shaded) required for perfect imaging. The pinhole size is extremely exaggerated for clarity of the wavefronts. The camera length  $L_i \gg a$ .

- Without a lens, a spherical wave of radius of curvature  $L_o$  diverging from the object  $P_0$  is incident on the pinhole and continues as a diverging wave toward the image plane at a distance  $L_i$  and forms a defocused image at  $P'_0$ .

Defocus wave aberration representing the sum of the sags of two spherical wavefronts passing through the center of the pinhole with their centers of curvature lying at the object and image points is given by

$$AB + BC = AC$$

or 
$$W(r_p) = \frac{1}{2} \left( \frac{1}{L_i} - \frac{1}{L_o} \right) r_p^2$$

where  $r_p$  is the radial distance of a point  $B$  in the plane of the pinhole from its center ( $L_o$  is numerically negative according to our sign convention).

- Image will be practically diffraction limited according to the *Rayleigh's quarter wave rule*, if the *peak value of defocus wave aberration is less than or equal to  $\lambda/4$* .

$$B_d = \frac{1}{2} \left( \frac{1}{L_i} - \frac{1}{L_o} \right) a^2 = \frac{\lambda}{4}$$

or  $\frac{1}{L_i} - \frac{1}{L_o} = \frac{\lambda}{2a^2} = \frac{1}{f_e}$

where  $f_e = 2a^2/\lambda$  is the effective focal length of the pinhole.

For a distant object ( $L_o \rightarrow -\infty$ ), we obtain

$$B_d = \frac{a^2}{2L_i} = \frac{\lambda}{4} \Rightarrow a = \sqrt{\lambda L_i / 2} \quad (\text{Same as the Petzval result})$$

The image spot for a point object is approximately the Airy disc with a radius of  $0.61\lambda L_i/a = 0.61\sqrt{2\lambda L_i}$ , or 0.61 times the value estimated by Petzval.

## Rayleigh approach (1891):

Axial irradiance of a beam at a distance  $z$  for a point source of intensity  $I_o$  diffracted by a circular aperture of radius  $a$ :

$$I(0; z) = \frac{P_{ex} S_{ex}}{\lambda^2 z^2} \left( \frac{\sin B_d/2}{B_d/2} \right)^2, \quad B_d(z) = \frac{\pi}{\lambda} \left( \frac{1}{z} - \frac{1}{R} \right) a^2 \rightarrow \frac{\pi}{\lambda} \left( \frac{1}{L_i} - \frac{1}{L_o} \right) a^2$$

$$P_{ex} = I_o \frac{\pi a^2}{L_o^2}, \quad I(0) = \frac{4I_o}{(L_i - L_o)^2} \sin^2 \left( \frac{\pi a^2}{2\lambda} \frac{L_i - L_o}{L_i L_o} \right)$$

For a given object distance  $L_o$ , *maximum central irradiance* at an image distance  $L_i$  is obtained when

$$\frac{\partial I(0)}{\partial L_i} = 0 \Rightarrow a = \sqrt{\lambda L_i} \Rightarrow \text{pinhole with one Fresnel zone}$$

Rayleigh concluded from his experimental observations that the best image was obtained when  $a_R = 0.95 \sqrt{\lambda L_i}$ , which is equivalent to the pinhole intercepting only 90% area of the first Fresnel zone.

## OTF approach:

*Defocus tolerance for Hopkins ratio*  $H(v) \gtrsim 0.8$  *for*  $v \lesssim 0.1$ :

$$B_d \lesssim \pm \lambda/20v = \lambda/2$$

$$B_d = \frac{a^2}{2L_i} \text{ for a distant object}$$

Hence,  $a = \sqrt{\lambda L_i}$  (same as Rayleigh's result)

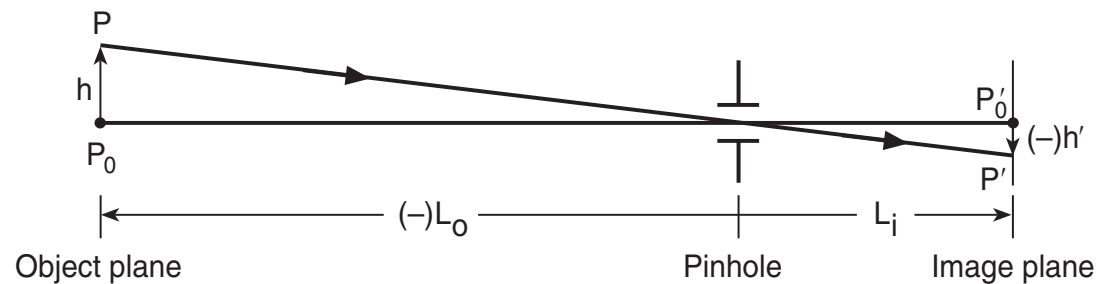
## Aberrations:

- Since the focal length  $f_e$  of the pinhole camera, approximately equal to  $2a^2/\lambda$ , depends on the wavelength, it suffers from *chromatic aberration*.
- Similarly, since the pinhole appears to be elliptical from an off-axis point object, its focal length for an object in the horizontal plane differs from that in a vertical plane. Hence, it suffers from *astigmatism*.

- It is *free of distortion*, i.e., the transverse image magnification  $M$  is independent of the field angle:

$$M = h'/h = L_i/L_o$$

The chief ray from an off-axis point object  $P$  at a height  $h$  (i.e., an object ray incident through the center of the pinhole) reaches the image plane at the image point  $P'$  at a height  $h'$  without any deviation, as illustrated below.



Distortion-free imaging

- *Disadvantage* of a pinhole camera is the *long exposure* it requires due to the small size of the pinhole.

## Two-Point Resolution

A measure of the imaging quality of a system is its ability to resolve closely-spaced objects.

**Rayleigh resolution:** Two point objects of equal intensity are just resolved if the principal maximum of the Airy pattern of one of them falls on the first zero of the other, i.e., if the separation between their Gaussian images is  $1.22\lambda F$ .

If the Gaussian images are located at  $x = \pm 0.61\lambda F$ , then the irradiance distribution of the aberration-free image along the  $x$  axis is given by

$$I(x) = \left\{ \frac{2J_1[\pi(x - 0.61)]}{\pi(x - 0.61)} \right\}^2 + \left\{ \frac{2J_1[\pi(x + 0.61)]}{\pi(x + 0.61)} \right\}^2$$

where  $x$  is in units of  $\lambda F$

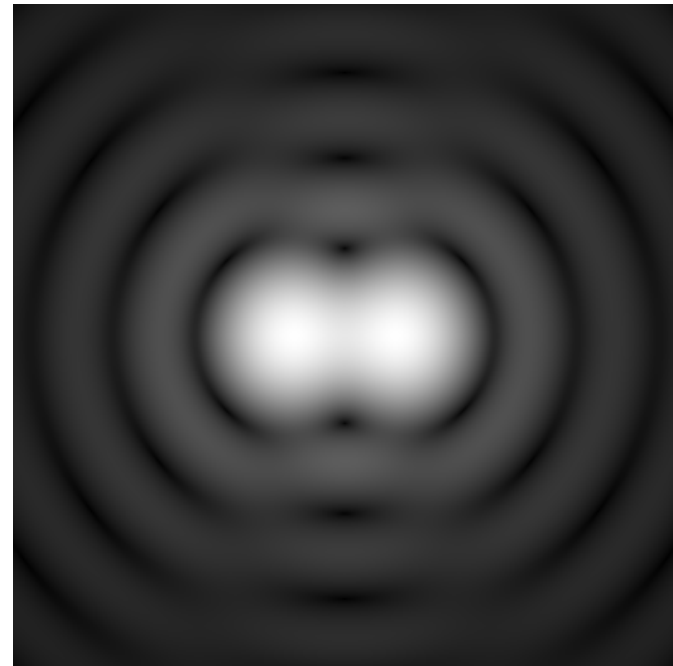
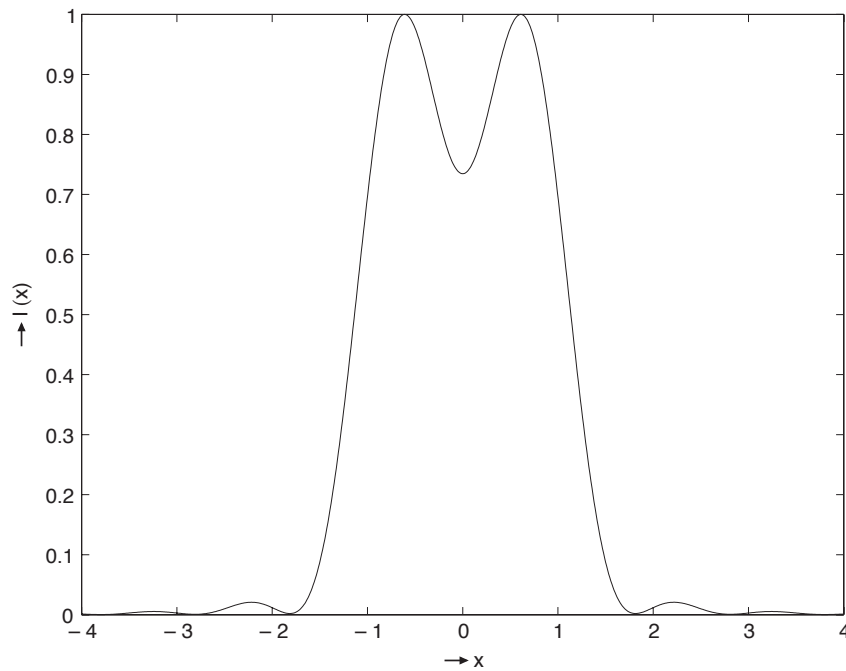


Figure 2-81. Irradiance distribution along the  $x$  axis of the **aberration-free** image of two *incoherent* point objects of equal intensity separated by the Rayleigh resolution of  $1.22\lambda F$ .  $x$  is in units of  $\lambda F$ .

- The dip at the center has a value of 0.73, compared to a maximum value of unity at  $x = \pm 0.61$ .

- Aberration-free image of a point object:

$$I(r) = \left[ \frac{2J_1(\pi r)}{\pi r} \right]^2$$

- Defocused image of a point object:

$$I(r; B_d) = 4 \left| \int_0^1 \exp(iB_d \rho^2) J_0(\pi r \rho) \rho d\rho \right|^2$$

- Defocused image of two incoherent point objects of equal intensity separated by the Rayleigh resolution of  $1.22\lambda F$  along the line passing through them, namely the  $x$  axis:

$$I(x; B_d) = 4 \left[ \left| \int_0^1 \exp(iB_d \rho^2) J_0[\pi(x - 0.61)\rho] \rho d\rho \right|^2 + \left| \int_0^1 \exp(iB_d \rho^2) J_0[\pi(x + 0.61)\rho] \rho d\rho \right|^2 \right]$$

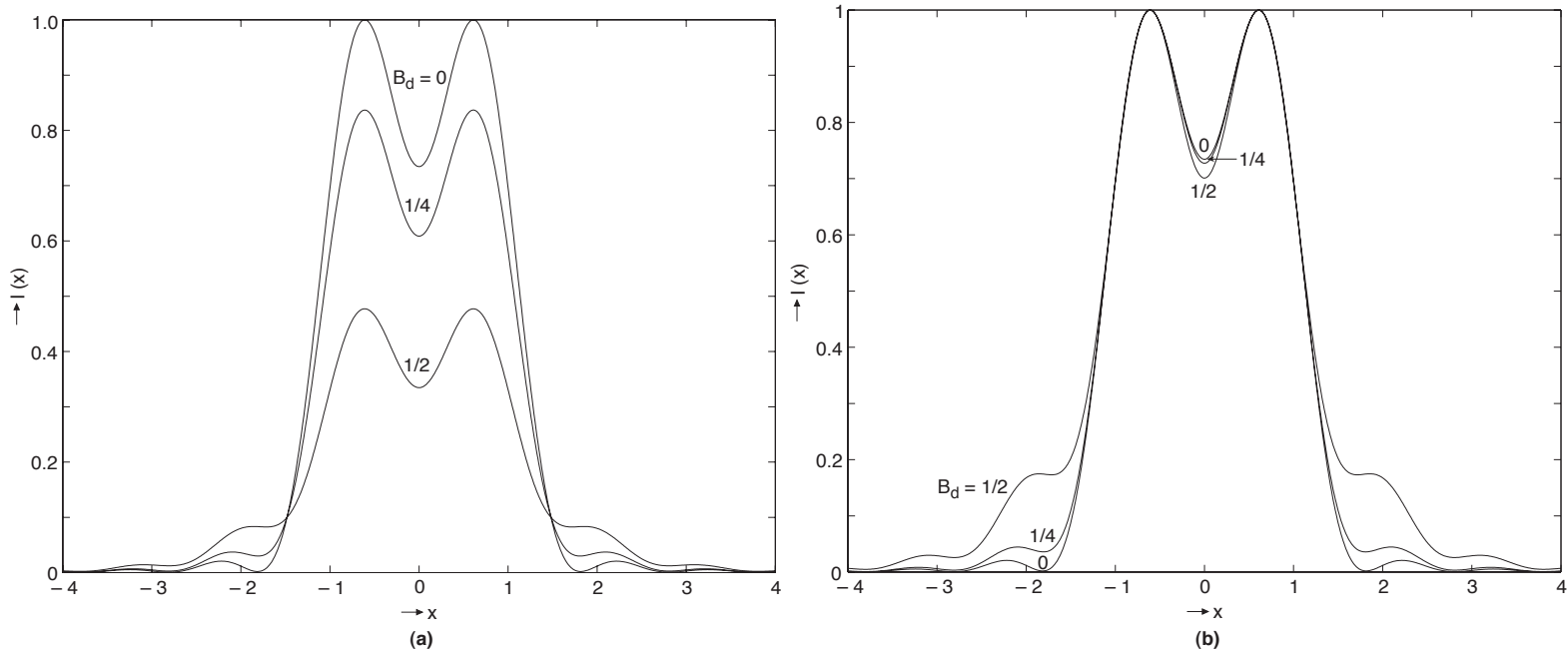
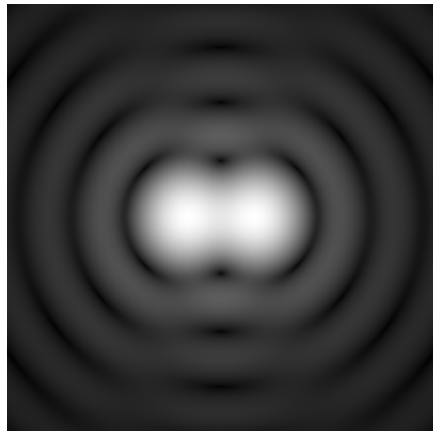
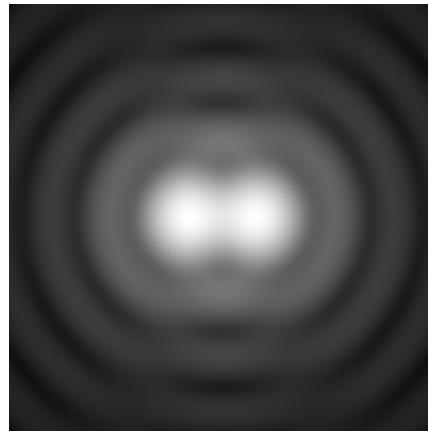


Figure 2-83. (a) **Defocused** image of two *incoherent* point objects separated by the Rayleigh resolution of  $1.22\lambda F$ .  $B_d$  is in units of  $\lambda$  and  $x$  is in units of  $\lambda F$ . (b) Distributions in (a) are normalized to unity at the principal peaks.

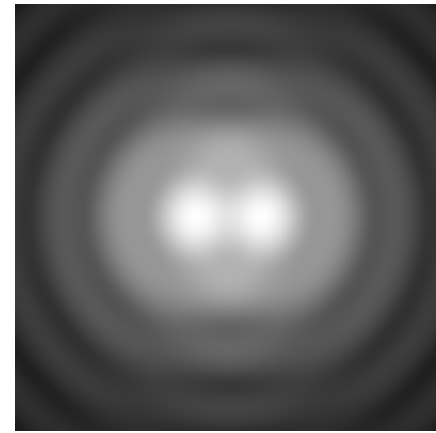
- Central values in (a) with increasing defocus are 0.73, 0.61, and 0.33, and the principal peaks have a value of 1, 0.84, and 0.48 located at  $x = \pm 0.61$ .
- Normalization of principal peaks to unity in (b) shows that the effect of defocus on the relative dip is small.



$$B_d = 0$$



$$B_d = 1/4$$



$$B_d = 1/2$$

Figure 2-85. Aberration-free and defocused images two incoherent point objects separated by the Rayleigh resolution.

- If the two point objects are **coherent** and in phase, they cannot be resolved.
- If they are not in phase, then their image appears as if they are of unequal intensities. See Figures 2-84 to 2-86.

## Mid Term Test